Apical SK potassium channels and Ca^{2+}-dependent anion secretion in endometrial epithelial cells

Melissa L. Palmer, Katherine R. Schiller and Scott M. O'Grady

Departments of Integrative Biology and Physiology and Department of Animal Science, 495 Animal Science/Veterinary Medicine Bldg, University of Minnesota, 1988 Fitch Avenue, St Paul, MN 55108, USA

Apical uridine triphosphate (UTP) stimulation was shown to increase short circuit current (I_{sc}) in immortalized porcine endometrial gland epithelial monolayers. Pretreatment with the bee venom toxin apamin enhanced this response. Voltage-clamp experiments using amphotericin B-permeablized monolayers revealed that the apamin-sensitive current increased immediately after UTP stimulation and was K^+ dependent. The current–voltage relationship was slightly inwardly rectifying with a reversal potential of -52 ± 2 mV, and the P_K/P_{Na} ratio was 14, indicating high selectivity for K^+. Concentration–response relationships for apamin and dequalinium had IC_{50} values of 0.5 nM and 1.8 μM, respectively, consistent with data previously reported for SK3 channels in excitable cells and hepatocytes. Treatment of monolayers with 50 μM BAPTA-AM completely blocked the effects of UTP on K^+ channel activation, indicating that the apamin-sensitive current was also Ca^{2+} dependent. Moreover, channel activation was blocked by calmidazolium ($IC_{50} = 5$ μM), suggesting a role for calmodulin in Ca^{2+}-dependent regulation of channel activity. RT-PCR experiments demonstrated expression of mRNA for the SK1 and SK3 channels, but not SK2 channels. Treatment of monolayers with 20 nM oestradiol-17β produced a 2-fold increase in SK3 mRNA, a 2-fold decrease in SK1 mRNA, but no change in GAPDH mRNA expression. This result correlated with a 2.5-fold increase in apamin-sensitive K^+ channel activity in the apical membrane. We speculate that SK channels provide a mechanism for rapidly sensing changes in intracellular Ca^{2+} near the apical membrane, evoking immediate hyperpolarization necessary for increasing the driving force for anion efflux following P2Y receptor activation.

(Resubmitted 9 August 2007; accepted after revision 22 November 2007; first published online 29 November 2007)
Corresponding author S. M. O'Grady: Departments of Physiology and Animal Science, 495 Animal Science/Veterinary Medicine Bldg, University of Minnesota, 1988 Fitch Ave., St Paul, MN 55108, USA. Email: ograd001@umn.edu

Small-conductance calcium-activated K^+ (SK) channels have been extensively studied in the nervous system where they play an important role in electrical signalling and regulation of intracellular Ca^{2+} ($[Ca^{2+}]_i$) (Stocker, 2004; Bond *et al.* 2005; Faber & Sah, 2007). Three SK channel subtypes, designated as SK1 (KCa2.1; KCNN1), SK2 (KCa2.2; KCNN2) and SK3 (KCa2.3; KCNN3) have been identified and cloned (Kohler *et al.* 1996; Shmukler *et al.* 2001; Stocker, 2004). SK channels are activated by relatively low concentrations of $[Ca^{2+}]_i$ (<500 nM), and analysis of the Hill coefficients obtained from Ca^{2+} concentration–effect relationships indicates the existence of multiple binding sites with a high degree of cooperativity (Xia *et al.* 1998; Hirschberg *et al.* 1999). Studies using excised patches indicate that Ca^{2+}-induced activation occurs at a rate similar to that of ligand-gated ion channels, indicating that SK channels rapidly sense and respond to changes in $[Ca^{2+}]_i$. Interestingly, SK channel activation is not mediated by direct binding of Ca^{2+} to the channel, but instead involves binding to calmodulin (CaM) which constitutively interacts with a specific binding domain (CaMBD) located near the S6 segment in each channel subunit (Xia *et al.* 1998).

Several pharmacological agents have been shown to inhibit the activity of SK channels (Grunnet *et al.* 2001*b*; Dale *et al.* 2002; Blank *et al.* 2004). For example, organic compounds including quaternary salts of bicuculline and dequalinium, along with various tricyclic antidepressants and antipsychotic phenothiazines have been shown to inhibit SK channels (Strobaek *et al.* 2000; Grunnet *et al.* 2001*b*; Liegeois *et al.* 2003; Terstappen *et al.* 2003). Perhaps the most widely used SK channel inhibitor is apamin, an 18-amino-acid peptide isolated from bee venom (Stocker *et al.* 1999; Strobaek *et al.* 2000; Grunnet *et al.* 2001*a*; Dale *et al.* 2002; D'Hoedt *et al.* 2004). Apamin is a potent and highly selective blocker of SK1, 2 and 3 channels, with K_D values ranging between 0.05 and 25 nM, depending on the isoform.

DOI: 10.1113/jphysiol.2007.142877

In the brain, small-conductance Ca^{2+}-activated K^+ channels are important regulators of excitability, and have distinct functional roles depending on the neuronal population in which they are expressed (Kohler *et al.* 1996; Bond *et al.* 2005). SK3 channels in particular have been shown to be expressed in other types of excitable cells including neurosecretory cells within the preoptic area of the rostral hypothalamus that produce gonadotropin-releasing hormone (GnRH) (Tse & Hille, 1992; Van Goor *et al.* 2000; Kato *et al.* 2006). SK3 channels have also been identified in smooth muscle cells including coronary smooth muscle, where they are involved in modulating the release of endothelial-derived hyperpolarization factor (Eichler *et al.* 2003), colonic smooth muscle (Ro *et al.* 2001), and uterine smooth muscle where they participate in the rhythmic contractions that occur during birth (Bond *et al.* 2000; Ro *et al.* 2001; Brown *et al.* 2007). SK2 and SK3 channels have been identified functionally in hepatocytes and hepatobiliary cell lines, particularly the SK3 isoform in rat liver (Barfod *et al.* 2001). Expression of all three SK family members was detected in both anterior and equatorial lens epithelial cells by PCR (Rhodes *et al.* 2006). Despite these recent studies however, little is known about the functional role of SK channels in native epithelial cells.

Previous measurements of uterine fluid ionic concentrations indicate that $[K^+]$ is elevated and $[Na^+]$ is reduced relative to plasma for these ions (Casslen & Nilsson, 1984; Iritani *et al.* 1974). These findings suggest that the endometrial epithelium is capable of K^+ secretion, but the transport and regulation mechanisms responsible for this process have not been characterized. In the present study, we investigated the effects of P2Y receptor stimulation on apical membrane K^+ channel function, using an immortalized endometrial epithelial cell line that exhibits Ca^{2+}-dependent anion secretion. Our initial experiments revealed that addition of UTP to the apical bathing solution produced activation of a Ca^{2+}-dependent K^+ conductance that was blocked by apamin. Additional experiments were performed to determine (1) the molecular identity of this Ca^{2+}-activated K^+ channel using molecular and pharmacological approaches; (2) the selectivity properties of the channel; and (3) the regulation of mRNA and functional expression by oestrogen. The results indicate that SK channels are activated in response to increases in intracellular calcium and that mRNA expression and transport activity are regulated by oestrogen.

Methods

Materials

Uridine triphosphate (UTP), 1,2-bis(2-aminophenoxy) ethane *N*,*N*,*N*′,*N*′-tetraacetic acid tetrakis (acetoxymethyl ester) (BAPTA-AM), dequalinium chloride, oestradiol-17β, progesterone, insulin, indometacin, amphotericin B, non-essential amino acid and high-purity-grade salts were purchased from Sigma Chemical Co (St Louis, MO, USA). Apamin and calmidazolium were obtained from Biomol (Plymouth Meeting, PA, USA). NPPB (5-nitro-2-(3-phenylpropylamino)-benzoate) was purchased from Calbiochem (San Diego, CA, USA). Semi-quantitative PCR and reverse transcription reagents were purchased from Invitrogen (Carlsbad, CA, USA). The DNA polymerase AmpliTaq Gold was purchased from Applied Biosystems (Foster City, CA, USA). PCR primers were synthesized by IDT (Coralville, IA, USA). All quantitative reverse transcriptase PCR (QRT-PCR) reagents were purchased from Stratagene (La Jolla, CA, USA). DNase-free RNA isolated from porcine brain was purchased from BioChain Institute Inc. (Hayward, CA, USA). Dulbecco's modified Eagle's medium (DMEM), Dulbecco's phosphate buffer saline (DPBS), fetal bovine serum (FBS), kanamycin and penicillin-streptomycin were purchased from Gibco BRL (Grand Island, NY, USA).

Cell culture

Immortalized porcine endometrial epithelial cells (PEG cells, passages 18–30) were propagated in DMEM supplemented with 1% L-glutamine, kanamycin, penicillin-streptomycin, non-essential amino acid and 10% fetal bovine serum as previously described (Palmer *et al.* 2006). PEG cells were seeded onto 4.5 cm^2 Transwell filters (Costar, Corning Incorporated, Acton, MA, USA), where they formed tight junctions, established polarity and attained a high transepithelial resistance. Once confluent monolayers were established, cells were maintained under serum-free conditions in the absence or presence of 20 nM oestradiol-17β, for 4 days prior to experimentation.

Measurement of monolayer electrical properties

Transepithelial resistance of the cell monolayers was measured using the EVOM epithelial voltohmeter coupled to Ag/AgCl 'chopstick' electrodes (World Precision Instruments (WPI), New Haven, CT, USA). High-resistance monolayers ($\sim$3000 Ω cm^2) were mounted in Ussing chambers, bathed on both sides with standard porcine saline solution containing (mM): 130 NaCl, 6 KCl, 1.5 $CaCl_2$, 1 $MgCl_2$, 20 $NaHCO_3$, 0.3 $Na H_2PO_4$, 1.3 Na_2HPO_4, pH 7.4, which was maintained at 37°C and bubbled with 95% O_2/5% CO_2. Transepithelial potential difference, monolayer conductance and short circuit current (I_{sc}) were measured with the use of voltage-clamp circuitry (DVC-1000) from WPI. The data from the voltage-clamp experiments were digitized,

stored and analysed using Axoscope software (Molecular Devices, Sunnyvale, CA, USA). All cells were pretreated with indometacin (10 μM) added to both apical and basolateral solutions at least 10 min before the beginning of the experiment.

For experiments involving measurement of membrane conductance, amphotericin B (15 μM) was used to permeablize the basolateral membrane of monolayers mounted in Ussing chambers. For experiments reported in Fig. 2, permeablized monolayers were bathed on the apical (extracellular) side with methane sulphonate ($MeSO_4$) saline solution containing (mM): 130 $NaMeSO_4$, 5 KCl, 20 $NaHCO_3$, 1 $MgSO_4$, 0.3 NaH_2PO_4, 2 calcium gluconate, 30 mannitol, 10 D-glucose (pH 7.4), while the basolateral surface was bathed with intracellular solution containing (mM): 130 $KMeSO_4$, 10 NaCl, 20 $KHCO_3$, 1 $MgSO_4$, 0.3 KH_2PO_4, 2 calcium gluconate, 30 mannitol, 10 D-glucose (pH 7.4). For experiments presented in Fig. 5, changes in extracellular $[K^+]$ were accomplished by partial replacement of $NaMeSO_4$ with 10, 35 or 95 mM $KMeSO_4$ in the apical solution. The data were digitized using a Digidata 1320 data acquisition system (Molecular Devices, Sunnyvale, CA, USA). Voltage step commands and the resultant currents were generated and recorded using pCLAMP 9 software (Molecular Devices, Sunnyvale, CA, USA). Current–voltage relationships were obtained by a series of voltage step commands described in the Results. The apamin-sensitive current components were obtained by subtracting currents before and after addition of 100 nM apamin. Electrophysiological experiments were performed at 37°C in HCO_3-containing bathing solutions gassed with 95% O_2/5% CO_2, pH = 7.4. The P_K/P_{Na} permeability ratio for the apamin-sensitive conductance was calculated from the reversal potential reported in Fig. 4*A*, using the bi-ionic equation (z = valence; F = Faraday's constant; E_{rev} = reversal potential; R = gas constant; T = absolute temperature, °K):

$$(P_K/P_{Na} = \left([Na^+]_i/[K^+]_o\right)\exp(zFE_{rev}/RT)$$

RT-PCR experiments

Total RNA from oestrogen-treated and serum-free PEG monolayers was extracted using cell lysis buffer RLT (Qiagen, Valencia, CA, USA), followed by mRNA enrichment using the RNeasy Mini kit (Qiagen,Valencia, CA, USA). Reverse transcription reactions were performed to generate complimentary DNA (cDNA) using 0.5 μg DNase-treated mRNA, 1 μl random hexamers (heated at 70°C for 10 min with mRNA in a 12 μl total reaction volume), 1 μl 10 mM dNTPs, 2 μl 0.1 M dTT, 4 μl 5× synthesis buffer and 1 μl reverse transcriptase in a 20 μl reaction volume. RT reactions were incubated for 52 min at 42°C, followed by 15 min at 75°C. Semi-quantitative PCR results were obtained using primers based on the porcine SK1, SK2, SK3 and internal control GAPDH gene products (SK1: forward primer: 5′ GCA CAA CTT CAT GAT GGA CA-3′, reverse primer: 5′-GAA CTT ACG CTG GTG TTT CC-3′; SK2: forward primer: 5′-CCC CGA GAT CGT GGT GTC TAA GC-3′, reverse primer: 5′-CAC ACA CCA GTA TTT CCA AGC AGA TG-3′; SK3: forward primer: 5′-TCC ATG TTT TCG TTG GCC CTG-3′, reverse primer: 5′ AGC ATG ACT CGG GCG ATC AGG TA-3′; GAPDH: forward primer: 5′-GAC CAC TTC GTC AAG CTC ATT TCC-3′, reverse primer: 5′-GAT GGT ACA TGA CGA GGC AGG TC-3′. Semi-quantitative PCR products were generated using 5 μl 10× PCR buffer, 1.5 μl 50 mM $MgCl_2$, 1 μl 10 mM dNTP mix, 1 μl each of the forward and reverse specific primers (10 μM) (see above), 0.4 μl DNA polymerase (Ambion), 2 μl of cDNA in a 50 μl total reaction volume. RT reactions were performed with a GeneAmp 9700 thermal cycler from Applied Biosystems (Foster City, CA, USA), using the following cycling conditions: 1 cycle to warm and hold at 94°C for 4 min; 40 cycles of 94°C for 45 s, 60°C for 45 s, 72°C for 1 min; followed by a final end cycle at 72°C for 7 min. Either 50 bp or 100 bp DNA markers were used to compare relative sizes of the PCR products. A single band was identified that matched the predicted size and sequence of the gene product. Densitometry analysis using Image J software (available from the NIH http://rsb.info.nih.gov/ij/download.html) was used to compare levels of PCR product in each lane. GAPDH was used as an internal control.

Quantitative (Q)RT-PCR was performed using the same primers for porcine SK3 and GAPDH (see above) using a Mx3005P Real-Time PCR machine from Stratagene (La Jolla, CA, USA). PCR reactions were performed with 12.5 μl 2× SYBR Green master mix, 0.375 μl passive reference dye (1 : 500), 1 μl of cDNA, 1 μl each of specific forward and reverse primers in a 25-μl reaction volume using the following cycling conditions: 95°C for 10 min followed by 40–50 cycles of 95°C 30 s, 60°C 45 s, 68°C 1 min; then to generate a dissociation curve: 95°C for 1 min and 59°C for 30 s. The dissociation curves consisted of a single sharp peak (Fig. 7*B*), indicating a unique PCR product for both SK3 and GAPDH.

Statistics

All values are presented as the mean ± S.E.M., where n represents the number of monolayers used in each experiment. The differences between control and treatment means were analysed using a two-tailed t test for unpaired means. A value of $P < 0.05$ was considered statistically significant.

Results

The effect of apical UTP on I_{sc} of monolayers treated with 20 nM oestradiol-17β for 4 days is shown in Fig. 1.

The UTP response was enhanced when monolayers were first treated with 100 nM apamin for 10 min prior to stimulation. The peak current was attained within 1 min after UTP addition and the increase in I_{sc} was persistent for more than 10 min. Subsequent experiments designed to measure changes in apical membrane conductance in oestradiol-treated monolayers showed that apical UTP elicited an immediate increase in inward current (Fig. 2*A*). Pretreatment of monolayers with the membrane-permeable calcium-chelating agent BAPTA-AM (50 μM) for 10 min abolished the UTP-stimulated inward current in each case, indicating a dependence on intracellular Ca^{2+} mobilization. Pretreatment with BAPTA-AM also reduced the rate of increase and the maximum UTP-stimulated outward current compared to control monolayers. It is worth noting that previous measurements of $[Ca^{2+}]_i$ demonstrated that pretreatment with 50 μM BAPTA-AM was sufficient to inhibit the increase in $[Ca^{2+}]_i$ produced by apical UTP in PEG cells (Palmer-Densmore *et al.* 2002). Inhibition of the outward current was attempted by using a known Cl^- channel inhibitor (200 μM NPPB). NPPB reduced the UTP-stimulated inward current and produced a similar initial effect as BAPTA-AM on the outward current, but inhibited the sustained component of the outward current. Thus the presence of this contaminating outward current limited our ability to characterize the steady-state properties of the apamin-sensitive conductance. Previous studies have reported that NPPB can inhibit SK4 channels and cardiac Na^+ channels at concentrations typically used to inhibit anion channels (Zhou *et al.* 2005; Fioretti *et al.* 2004). Therefore, we suggest that inhibition of the inward current presented in Fig. 2 represents a non-specific effect of NPPB on SK channel activity in PEG cells.

The effect of SK channel inhibitors on the apical UTP-activated inward current is presented in Fig. 3. Apamin and dequalinium each inhibited approximately 80% of the current, and their effects were non-additive. This could have resulted from incomplete block by these inhibitors or suggests the possibility that another Ca^{2+}-dependent K^+ channel is responsible for a small portion of the inward current. Analysis of the concentration–response relationships revealed IC_{50}

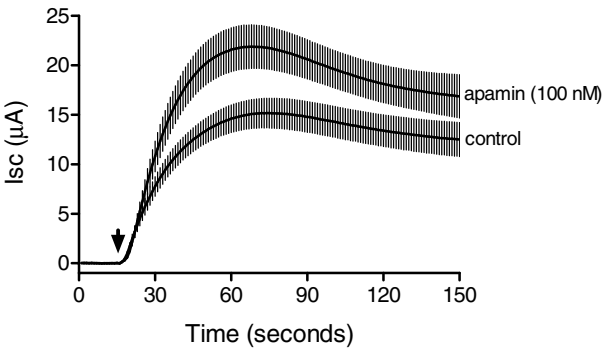

Figure 1. These results show the effect of apical UTP (0.5 μM) on I_{sc} of monolayers cultured in the presence of 20 nM oestradiol-17β for 4 days prior to experimentation
Pretreatment with apamin (100 nM) for 10 min before adding UTP to the apical solution resulted in a significant increase in the peak I_{sc} (UTP was added at 15 s and the peak I_{sc} was measured at 70 s) compared to control monolayers. The mean digitized tracings of six control and six apamin-treated monolayers are shown along with standard error values (vertical bars) for each of the data points.

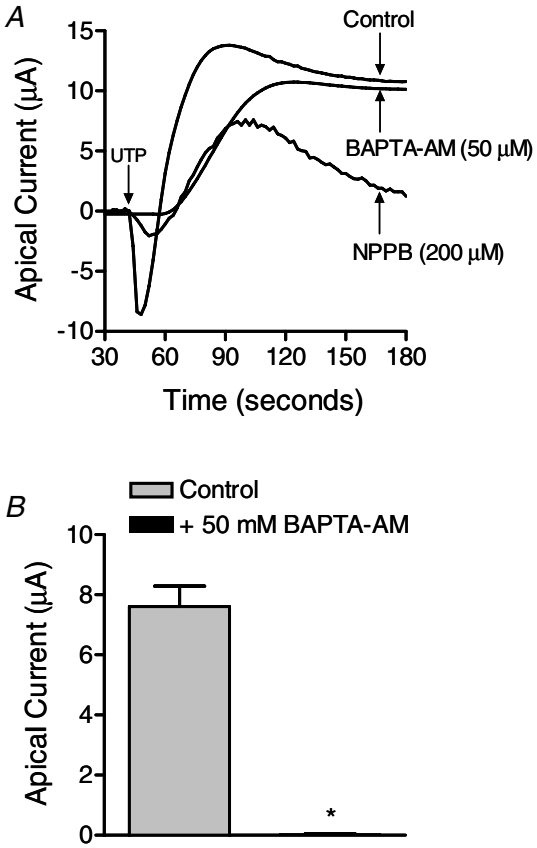

Figure 2. The effects of UTP and BAPTA-AM on apical membrane current of amphotericin B-permeablized monolayers maintained in the presence of 20 nM oestradiol-17β for 4 days
A, monolayers stimulated with apical UTP (10 μM) exhibited a rapid increase in inward current consistent with movement of K^+ down its concentration gradient. The tracing is representative of data from 16 monolayers. Treatment with BAPTA-AM abolished the initial inward current response elicited by UTP and reduced the rate at which outward current developed after stimulation with UTP ($n = 5$). Attempts to block the outward current by pretreatment with 200 μM NPPB resulted in a decrease in inward current and a reduction in outward current following stimulation with UTP ($n = 3$). *B*, bar graph showing the peak inward current elicited by UTP in the absence and presence of 50 μM BAPTA-AM. The data represent the mean ± S.E.M. from 16 control and 5 BAPTA-AM-pretreated monolayers (*indicates a significant decrease in peak inward current compared to control monolayers).

values of 0.50 ± 0.02 nM (Hill slope $= -0.82 \pm 0.08$) for apamin and $1.8\ \mu$M ± 0.09 (Hill slope $= -1.08 \pm 0.12$) for dequalinium (Fig. 3*B*). Previous studies have shown that Ca^{2+} regulation of SK channel activity is dependent on calmodulin, which is constitutively bound to the channel. To determine whether an interaction with calmodulin was necessary for channel activation in PEG cells, monolayers were pretreated with the membrane-permeable calmodulin antagonist, calmidazolium. Calmidazolium produced a concentration-dependent inhibition of inward current with an IC_{50} of $5 \pm 0.11\ \mu$M (Hill slope $= -2.0 \pm 0.1$), consistent with its effects on calmodulin (Fig. 4).

The ion selectivity of the apamin-sensitive conductance is described in Fig. 5. Monolayers were permeablized with $15\ \mu$M amphotericin B added to the basolateral solution to eliminate the basolateral membrane as a resistive barrier. The ionic compositions of the apical and basolateral solutions are given in the Methods. The current–voltage relationship was measured at the peak of the inward current at a holding potential of 0 mV, using a series of voltage steps from -100 to $+40$ mV in 20 mV increments (duration $= 200$ ms step^{-1}, total protocol duration $= 2.4$ s) in the presence and absence of 100 nM apamin. The apamin-sensitive current–voltage relationship exhibited a slight inward rectification with a reversal potential of -52 ± 2 mV (Fig. 5*A*). The P_K/P_{Na} permeability ratio as calculated using the bi-ionic equation presented in the Methods was equal to 14. The reversal potential was also shown to be dependent on extracellular $[K^+]$ as shown in Fig. 5*B*. The slope of the reversal potential *versus* log $[K^+]_o$ relationship was 50 mV/(10-fold change in $[K^+]_o$).

RT-PCR was used to identify SK channel subtype expression in PEG cells. In control experiments DNase-treated RNA samples from porcine brain were used as a positive control to verify the detection of each of the SK channels using the primers described in the Methods (Fig. 6*A*). PCR products of appropriate size were detected for each primer set while no products were observed in the absence of template (nT) or when RNA was substituted for cDNA (No RT). Figure 6*B* shows the PCR products obtained from oestradiol 17β

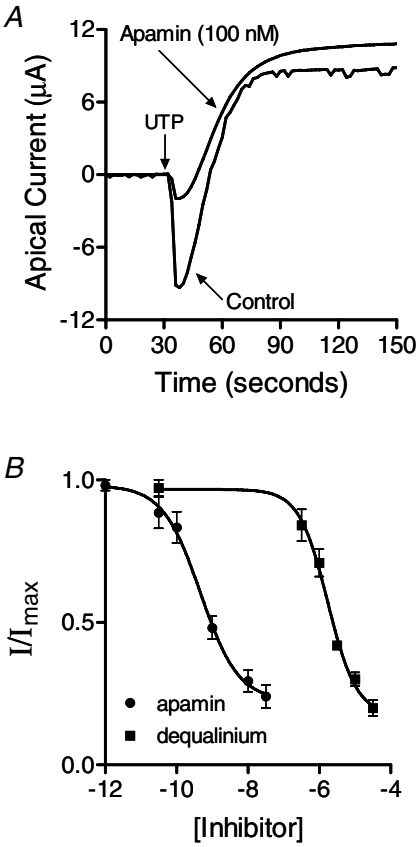

Figure 3 Effects of SK channel inhibitors on the UTP-activated K current
A, representative apical membrane current traces obtained from amphotericin B-permeablized monolayers maintained in the presence of 20 nM oestradiol-17β for 4 days with and without 100 nM apamin added to the apical solution ($n = 6$). *B*, concentration–response relationships for apamin and dequalinium where the peak inward current was measured in response to stimulation with UTP (10 μM) in amphotericin B-permeablized monolayers treated with oestradiol-17β. The data were fitted (PRISM: GraphPad Software Inc., San Diego CA) by a four parameter logistic function: $Y = \text{Min} + ((\text{Max} - \text{Min})/(1 + 10((\log IC_{50} - X)*n)))$ where Y = normalized current, X = log inhibitor concentration, n = Hill coefficient (equal to -0.82 ± 0.08 and -1.08 ± 0.12) for apamin and dequalinium, respectively) and the IC_{50} values were determined from the fit ($IC_{50} = 0.50 \pm 0.02$ nM ($n = 6$) and $1.8 \pm 0.09\ \mu$M ($n = 6$) for apamin and dequalinium, respectively).

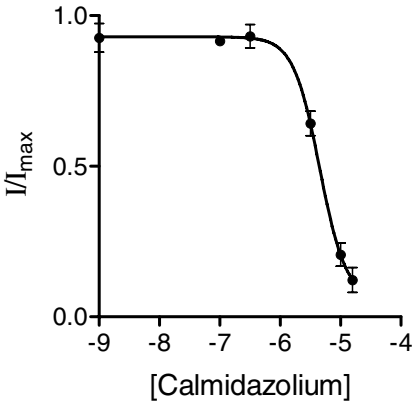

Figure 4. Effects of a calmodulin antagonist on the UTP-activated K^+ current
Pretreatment of monolayers (10 min) with calmidazolium produced a concentration-dependent inhibition of channel activity. Apical membrane currents were measured using amphotericin B-permeablized monolayers maintained in the presence of 20 nM oestradiol-17β for 4 days. The equation given above (Fig. 3*B*) was fitted to the data set to derive the following parameters: $IC_{50} = 5 \pm 0.11\ \mu$M; Hill coefficient $= -2.0 \pm 0.1$, $n = 5$.

(20 nM, 4 days)-treated monolayers using SK1–3 primers. RT-PCR reactions performed with cDNA synthesized from PEG cell mRNA revealed the presence of SK1 and SK3 PCR products, indicating that mRNA for both SK channel subtypes is expressed. Comparison of serum-free and oestrogen-treated (20 nM, 4 days) PEG cells showed a 2.3-fold increase in SK3 and a 1.9-fold decrease in SK1 mRNA expression as indicated by densitometry analysis following normalization to background and corresponding GAPDH controls (Fig. 6*C* and *D*).

Figure 7 shows the results of QRT-PCR experiments designed to measure the change in SK3 mRNA expression induced by oestradiol-17β (20 nM, 4 days). Analysis of the CT values (reported in the legend to Fig. 7) indicated that oestrogen treatment increases SK3 mRNA expression by 1.7 ± 0.17-fold. Analysis of the effects of oestrogen on the magnitude of apamin-sensitive apical membrane K^+ current showed an increase of 2.5-fold compared to serum-free control monolayers.

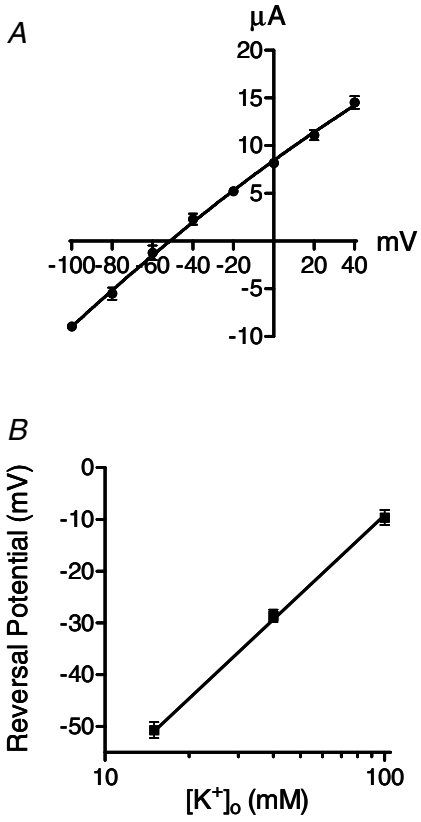

Figure 5. The selectivity properties of the UTP-activated, apamin-sensitive apical membrane conductance
A, current–voltage relationship of monolayers maintained in the presence of 20 nM oestradiol-17β for 4 days and bathed with an apical solution containing 15 mM $[K^+]$. The reversal potential was -52 ± 2 mV ($n = 4$). The current–voltage relationship exhibited slight inward rectification as revealed by attempting a linear fit over the entire range of values. A line connecting points between -40 mV and $+40$ mV failed to intersect data points between -60 mV and -100 mV, which deviated below the line by more than their S.E.M. values. *B*, effects of extracellular $[K^+]$ on reversal potential of the apamin-sensitive apical current ($n = 4$ at 15 mM $[K^+]$; $n = 6$ at 40 and 100 mM $[K^+]$).

Discussion

PEG cells express apical $P2Y_2$, $P2Y_4$ and $P2Y_6$ receptors that recognize ATP/UTP, UTP and UDP, respectively (Palmer *et al.* 2006). Previous studies have shown that stimulation with UTP produced an increase in I_{sc} that involved activation of apical Ca^{2+}-activated Cl^- channels and CFTR. The results of the present study extend these earlier observations by demonstrating that PEG cells express apical SK K^+ channels, which are activated following stimulation with UTP. Two known SK3 channel inhibitors, apamin and dequalinium, were shown to inhibit the UTP-activated K^+ current in a concentration-dependent manner, with IC_{50} values similar to published data on native channels in excitatory cells and expressed channels in HEK293 cells (Barfod *et al.* 2001; Grunnet *et al.* 2001*b*). The apamin-sensitive conductance present in the apical membrane of PEG cells was shown to be highly selective for K^+, with a P_K/P_{Na} ratio of 14 and 50 mV/(10 fold change in $[K]_o$), similar to previous findings obtained from expressed SK3 channels cloned from rat liver (Barfod *et al.* 2001).

The data presented in this study suggested that the apamin-sensitive K^+ conductance participates in K^+ secretion in PEG cells. This was inferred from experiments showing an increase in the UTP-stimulated I_{sc} following pretreatment with apamin. An enhanced I_{sc} response would be expected if K^+ secretion was occurring in parallel with anion secretion, since a portion of the UTP-stimulated current would appear electroneutral. Previous studies in pigs and humans have shown that uterine fluid has a higher K^+ concentration than plasma (Iritani *et al.* 1974; Casslen & Nilsson, 1984). Thus K^+ secretion mediated by SK channels in endometrial glands may contribute, in part, to the elevated $[K^+]$ observed in uterine fluid.

SK channel activation in PEG cells was completely inhibited after pretreatment with BAPTA-AM, demonstrating calcium dependence of the apamin-sensitive channels. Activation also required an interaction with calmodulin (CaM), as demonstrated by a concentration-dependent inhibition of channel function with the CaM-selective inhibitor, calmidazolium. Previously, a model for Ca^{2+} gating was proposed using rat SK channels, where calmodulin was constitutively bound to the calmodulin-binding domain (CaMBD) of the channel, essentially rendering the complex resistant to the actions of calmidazolium (Xia *et al.* 1998).

Comparison of the rat CaMBD with pig, human and mouse sequences shows that G606 in the rat is replaced with S in pig and in human (see Table 1).

We speculate that the ability of calmidazolium to interact with calmodulin in porcine SK channels may be due in part to a weaker interaction between CaMBD and calmodulin relative to interactions with rat or mouse SK channels. This diminished affinity may result from a single amino acid difference (G^{606} to S^{606}) in the C-terminal portion of the CaMBD, which is believed to interact with hydrophobic residues exposed by folding of the EF-hands motif of calmodulin. It is interesting to note that the RS606VK sequence in porcine and human SK3 may function as a phosphorylation site such that the presence of a phosphoserine may weaken the binding interaction between the CaMBD and CaM.

Oestrogen regulation of SK3 channel mRNA expression has been documented previously in native cells and in heterologous expression systems (Bosch *et al.* 2002; Jacobson *et al.* 2003; Kelly *et al.* 2002*a*, 2002*b*, 2003). Oestrogen treatment of ovariectomized guinea pigs was shown to increase SK3 channel mRNA levels in the rostral hypothalamus, a region that contains a large proportion of GnRH neurosecretory cells that are known to express oestrogen receptors (Bosch *et al.* 2002). Oestrogen was also shown to stimulate SK3 gene expression in rat myoblasts (L6 cells) and endogenous SK3 channel expression in Cos7 cells after transfection with oestrogen receptor α (ERα; Jacobson *et al.* 2003). In the study by Jacobson *et al.* (2003), a 33 bp enhancer sequence adjacent to the SK3 promotor was identified and shown to bind Sp1 and Sp3. Oestradiol-17β binding to the endogenous

Table 1. Pig, human, rat and mouse C-terminal portion of the CaMBD of SK3 channels

Species	C-terminal sequence
Pig	601 IHQLR**S**VKMEQRKLSDQANTLVDLSKMQ 628
Human	601 IHQLR**S**VKMEQRKLSDQANTLVDLSKMQ 628
Rat	601 IHQLR**G**VKMEQRKLSDQANTLVDLSKMQ 628
Mouse	601 IHQLR**G**VKMEQRKLSDQANTLVDLSKMQ 628

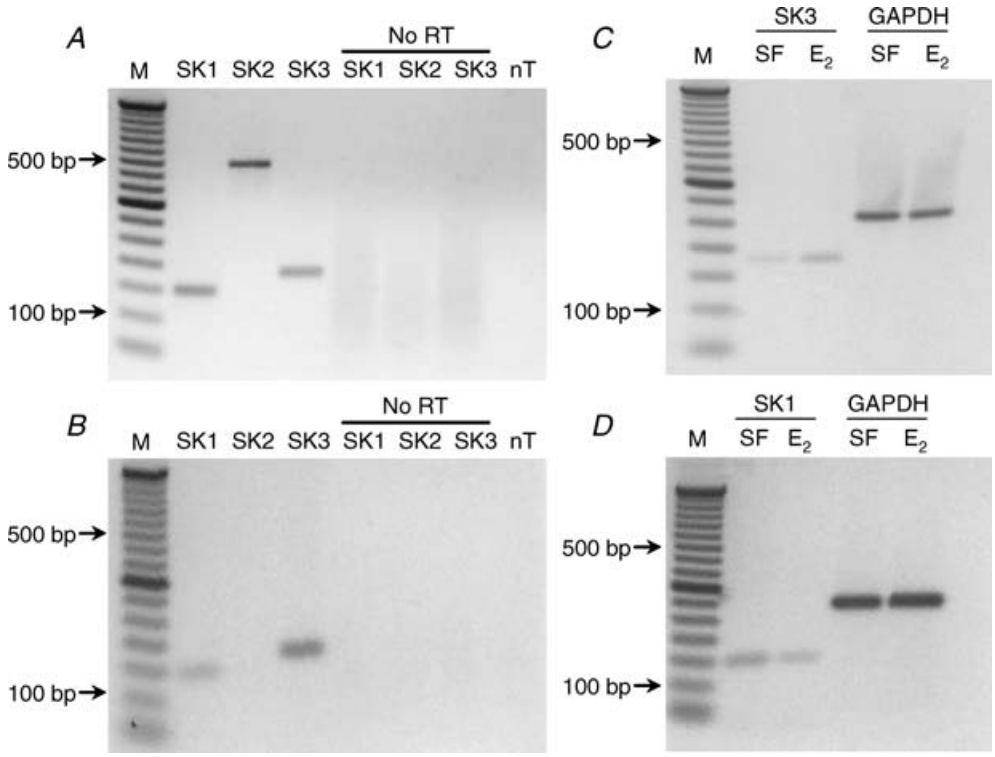

Figure 6. Molecular identification of SK1 and SK3 channel mRNA in porcine brain and PEG cells
A, PCR products (40 cycles) obtained from RT-PCR reactions performed using cDNA synthesized from DNase-treated mRNA isolated from porcine brain (primers are described in the Methods). Control: no RT reactions were performed using RNA instead of cDNA for each primer set. In the no template (nT) control, molecular biology grade water was used to replace the cDNA template. *B*, SK channel expression in immortalized PEG cells. SK1 and SK3 PCR products were detected at 40 cycles. Similar control reactions were performed as described in *A*. *C* and *D*, treatment with 20 nM oestradiol-17β for 4 days resulted in a 2.3-fold increase in SK3 mRNA expression and a 1.9-fold decrease in SK1 mRNA expression compared to serum-free controls as indicated by densitometry analysis (29 and 38 cycles, respectively). No difference in GAPDH mRNA expression was detected between serum-free and oestradiol-17β-treated monolayers.

ERα receptor in L6 cells was shown to increase the affinity of Sp1 for the enhancer and stimulate transcription. In the present study, messenger RNA levels of SK3 channels and corresponding functional activity increased following stimulation with oestradiol-17β, results consistent with the studies described above.

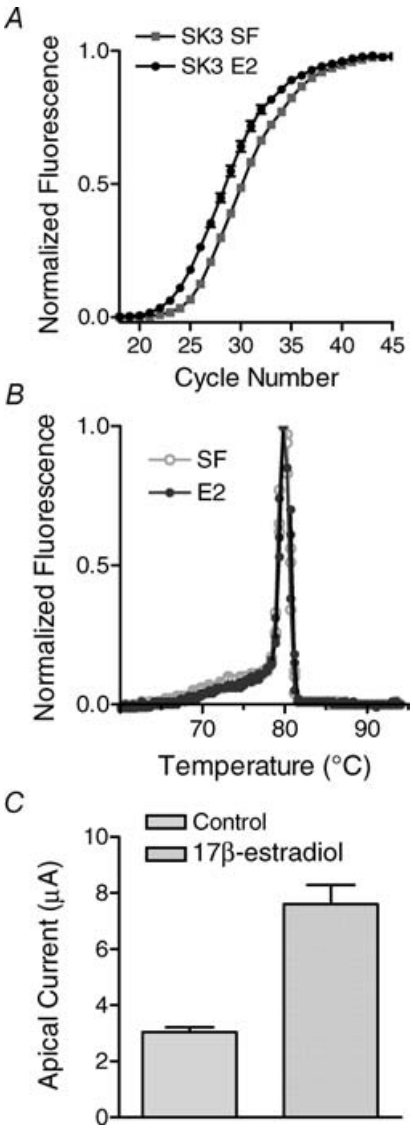

Figure 7. Quantitative RT-PCR analysis of SK3 mRNA expression and measurements of apamin-sensitive apical membrane current in immortalized PEG cells
A, amplification plots showing SK3 mRNA expression in confluent PEG cell monolayers under serum-free and oestrogen (E2, 20 nM, 4 days)-stimulated conditions ($n = 3$ for each condition). CT values for SK3 were 26.62 $\pm$ 0.04 and 24.96 $\pm$ 0.09 for serum-free and E2-treated conditions, respectively (QRT-PCR reaction efficiency = 87% based on the slope of the linear portion of the amplification plot). *B*, temperature dissociation plot for serum-free and oestradiol-treated samples used for generating the amplification plot shown in *A* ($n = 3$ for each condition). Note that a single peak was detected indicating that a unique PCR product was obtained. *C*, comparison of maximum UTP-stimulated, apamin-sensitive (100 nM), apical membrane currents of monolayers maintained for 4 days under serum-free conditions or in the presence of 20 nM oestradiol-17β. Monolayers treated with oestradiol exhibited a 2.5-fold greater apamin-sensitive inward current following stimulation with UTP (10 μM).

Recent coexpression studies of SK1 and SK3 channels in a heterologous cell system suggested that coassembly of SK1 and SK3 subunits occurs but that SK channel activity is inhibited (Monaghan *et al.* 2004). Immunohistochemical data indicated that coassembly appeared to inhibit trafficking of heteromeric channels to the membrane. The fact that PEG cells express both SK1 and SK3 channel mRNA suggests the possibility that coassembly of these subunits may occur, but that these heteromeric channels may not traffic to the apical membrane. Our finding that oestrogen stimulated SK3 but reduced SK1 channel mRNA expression suggests the possibility that a decrease in the number of SK1 subunits may enhance the membrane surface expression of SK3 channels and by this means, increase channel activity. Although this is an intriguing speculation, it is difficult to say whether it contributes to enhanced functional activity of SK3 channels in oestrogen-treated PEG cells, since we do not know whether heteromeric SK1/SK3 channels form in porcine cells or exhibit altered membrane trafficking properties. Thus additional studies will be necessary to determine the physiological role of SK1 channels in epithelial cells.

In conclusion, we have identified an apamin-sensitive, slightly inwardly rectifying, Ca^{2+}/calmodulin-activated K^+ conductance in the apical membrane of immortalized PEG cells that opens in response to P2Y receptor stimulation with UTP. Pharmacological studies and analysis of mRNA expression indicate that either SK1 (KCNN1) or SK3 (KCNN3) channel isoforms (or both) may be responsible for this UTP-stimulated increase in K^+ channel activity. These channels were found to be highly selective for K^+, consistent with previously published data from excitatory and non-excitatory cell types. In PEG cells, the effect of apical apamin on I_{sc} was consistent with a role for SK channels in K^+ secretion. Moreover, our results showed that BAPTA inhibited the UTP-induced transient inward current, suggesting that SK channels responded rapidly to changes in intracellular Ca^{2+}. Such an increase in apical K^+ conductance would be expected to produce membrane hyperpolarization, increasing the driving force for anion efflux across the apical membrane. Our finding that SK3 mRNA expression was stimulated by oestrogen and that oestrogen increased the apamin-sensitive current in response to UTP indicated that K^+ secretion may be subject to regulation during the oestrus cycle.

References

Barfod ET, Moore AL & Lidofsky SD (2001). Cloning and functional expression of a liver isoform of the small conductance Ca^{2+}-activated K^+ channel SK3. *Am J Physiol Cell Physiol* **280**, C836–C842.

Blank T, Nijholt I, Kye MJ & Spiess J (2004). Small conductance Ca^{2+}-activated K^+ channels as targets of CNS drug development. *Curr Drug Targets CNS Neurol Disord* **3**, 161–167.

Bond CT, Maylie J & Adelman JP (2005). SK channels in excitability, pacemaking and synaptic integration. *Curr Opin Neurobiol* **15**, 305–311.

Bond CT, Sprengel R, Bissonnette JM, Kaufmann WA, Pribnow D, Neelands T, Storck T, Baetscher M, Jerecic J, Maylie J, Knaus HG, Seeburg PH & Adelman JP (2000). Respiration and parturition affected by conditional overexpression of the Ca^{2+}-activated K^+ channel subunit, SK3. *Science* **289**, 1942–1946.

Bosch MA, Kelly MJ & Ronnekleiv OK (2002). Distribution, neuronal colocalization, and 17beta-E2 modulation of small conductance calcium-activated K^+ channel (SK3) mRNA in the guinea pig brain. *Endocrinology* **143**, 1097–1107.

Brown A, Cornwell T, Korniyenko I, Solodushko V, Bond CT, Adelman JP & Taylor MS (2007). Myometrial expression of small conductance Ca^{2+}-activated K^+ channels depresses phasic uterine contraction. *Am J Physiol Cell Physiol* **292**, C832–C840.

Casslen B & Nilsson B (1984). Human uterine fluid, examined in undiluted samples for osmolarity and the concentrations of inorganic ions, albumin, glucose, and urea. *Am J Obstet Gynecol* **150**, 877–881.

Dale TJ, Cryan JE, Chen MX & Trezise DJ (2002). Partial apamin sensitivity of human small conductance Ca^{2+}-activated K^+ channels stably expressed in Chinese hamster ovary cells. *Naunyn Schmiedebergs Arch Pharmacol* **366**, 470–477.

D'Hoedt D, Hirzel K, Pedarzani P & Stocker M (2004). Domain analysis of the calcium-activated potassium channel SK1 from rat brain. Functional expression and toxin sensitivity. *J Biol Chem* **279**, 12088–12092.

Eichler I, Wibawa J, Grgic I, Knorr A, Brakemeier S, Pries AR, Hoyer J & Kohler R (2003). Selective blockade of endothelial Ca^{2+}-activated small- and intermediate-conductance K^+-channels suppresses EDHF-mediated vasodilation. *Br J Pharmacol* **138**, 594–601.

Faber ES & Sah P (2007). Functions of SK channels in central neurons. *Clin Exp Pharmacol Physiol* **34**, 1077–1083.

Fioretti B, Castigli E, Calzuola I, Harper AA, Franciolini F & Catacuzzeno L (2004). NPPB block of the intermediate-conductance Ca^{2+}-activated K^+ channel. *Eur J Pharmacol* **497**, 1–6.

Grunnet M, Jensen BS, Olesen SP & Klaerke DA (2001*a*). Apamin interacts with all subtypes of cloned small-conductance Ca^{2+}-activated K^+ channels. *Pflugers Arch* **441**, 544–550.

Grunnet M, Jespersen T, Angelo K, Frokjaer-Jensen C, Klaerke DA, Olesen SP & Jensen BS (2001*b*). Pharmacological modulation of SK3 channels. *Neuropharmacology* **40**, 879–887.

Hirschberg B, Maylie J, Adelman JP & Marrion NV (1999). Gating properties of single SK channels in hippocampal CA1 pyramidal neurons. *Biophys J* **77**, 1905–1913.

Iritani A, Sato E & Nishikawa Y (1974). Secretion rates and chemical composition of oviduct and uterine fluids in sows. *J Anim Sci* **39**, 582–588.

Jacobson D, Pribnow D, Herson PS, Maylie J & Adelman JP (2003). Determinants contributing to estrogen-regulated expression of SK3. *Biochem Biophys Res Commun* **303**, 660–668.

Kato M, Tanaka N, Usui S & Sakuma Y (2006). The SK channel blocker apamin inhibits slow afterhyperpolarization currents in rat gonadotropin-releasing hormone neurones. *J Physiol* **574**, 431–442.

Kelly MJ, Qiu J & Ronnekleiv OK (2003). Estrogen modulation of G-protein-coupled receptor activation of potassium channels in the central nervous system. *Ann N Y Acad Sci* **1007**, 6–16.

Kelly MJ, Qiu J, Wagner EJ & Ronnekleiv OK (2002*a*). Rapid effects of estrogen on G protein-coupled receptor activation of potassium channels in the central nervous system (CNS). *J Steroid Biochem Mol Biol* **83**, 187–193.

Kelly MJ, Ronnekleiv OK, Ibrahim N, Lagrange AH & Wagner EJ (2002*b*). Estrogen modulation of K^+ channel activity in hypothalamic neurons involved in the control of the reproductive axis. *Steroids* **67**, 447–456.

Kohler M, Hirschberg B, Bond CT, Kinzie JM, Marrion NV, Maylie J & Adelman JP (1996). Small-conductance, calcium-activated potassium channels from mammalian brain. *Science* **273**, 1709–1714.

Liegeois JF, Mercier F, Graulich A, Graulich-Lorge F, Scuvee-Moreau J & Seutin V (2003). Modulation of small conductance calcium-activated potassium (SK) channels: a new challenge in medicinal chemistry. *Curr Med Chem* **10**, 625–647.

Monaghan AS, Benton DC, Bahia PK, Hosseini R, Shah YA, Haylett DG & Moss GW (2004). The SK3 subunit of small conductance Ca^{2+}-activated K^+ channels interacts with both SK1 and SK2 subunits in a heterologous expression system. *J Biol Chem* **279**, 1003–1009.

Palmer ML, Lee SY, Carlson D, Fahrenkrug S & O'Grady SM (2006). Stable knockdown of CFTR establishes a role for the channel in P2Y receptor-stimulated anion secretion. *J Cell Physiol* **206**, 759–770.

Palmer-Densmore M, Deachapunya C, Kannan M & O'Grady SM (2002). UTP-dependent inhibition of Na^+ absorption requires activation of PKC in endometrial epithelial cells. *J Gen Physiol* **120**, 897–906.

Rhodes JD, Monckton DG, McAbney JP, Prescott AR & Duncan G (2006). Increased SK3 expression in DM1 lens cells leads to impaired growth through a greater calcium-induced fragility. *Hum Mol Genet* **15**, 3559–3568.

Ro S, Hatton WJ, Koh SD & Horowitz B (2001). Molecular properties of small-conductance Ca^{2+}-activated K^+ channels expressed in murine colonic smooth muscle. *Am J Physiol Gastrointest Liver Physiol* **281**, G964–G973.

Shmukler BE, Bond CT, Wilhelm S, Bruening-Wright A, Maylie J, Adelman JP & Alper SL (2001). Structure and complex transcription pattern of the mouse SK1 K(Ca) channel gene, KCNN1. *Biochim Biophys Acta* **1518**, 36–46.

Stocker M (2004). Ca^{2+}-activated K^+ channels: molecular determinants and function of the SK family. *Nat Rev Neurosci* **5**, 758–770.

Stocker M, Krause M & Pedarzani P (1999). An apamin-sensitive Ca^{2+}-activated K^+ current in hippocampal pyramidal neurons. *Proc Natl Acad Sci U S A* **96**, 4662–4667.

Strobaek D, Jorgensen TD, Christophersen P, Ahring PK & Olesen SP (2000). Pharmacological characterization of small-conductance Ca^{2+}-activated K^+ channels stably expressed in HEK 293 cells. *Br J Pharmacol* **129**, 991–999.

Terstappen GC, Pellacani A, Aldegheri L, Graziani F, Carignani C, Pula G & Virginio C (2003). The antidepressant fluoxetine blocks the human small conductance calcium-activated potassium channels SK1, SK2 and SK3. *Neurosci Lett* **346**, 85–88.

Tse A & Hille B (1992). GnRH-induced Ca^{2+} oscillations and rhythmic hyperpolarizations of pituitary gonadotropes. *Science* **255**, 462–464.

Van Goor F, Krsmanovic LZ, Catt KJ & Stojilkovic SS (2000). Autocrine regulation of calcium influx and gonadotropin-releasing hormone secretion in hypothalamic neurons. *Biochem Cell Biol* **78**, 359–370.

Xia XM, Fakler B, Rivard A, Wayman G, Johnson-Pais T, Keen JE, Ishii T, Hirschberg B, Bond CT, Lutsenko S, Maylie J & Adelman JP (1998). Mechanism of calcium gating in small-conductance calcium-activated potassium channels. *Nature* **395**, 503–507.

Zhou SS, Yang J, Li YQ, Zhao LY, Xu M & Ding YF (2005). Effect of Cl^- channel blockers on aconitine-induced arrhythmias in rat heart. *Exp Physiol* **90**, 865–872.

Acknowledgements

The authors wish to thank Peter Maniak for technical assistance. This work was supported by funds from the National Institutes of Health, DK07401 to smo and from the Minnesota Agricultural Experiment Station, AES P82 to s.m.o.